Clinical Chemistry 59:4
641–648 (2013)

Lateral Flow Assay with Near-Infrared Dye for Multiplex Detection

Christina Swanson,[1*] and Annalisa D'Andrea[1*]

BACKGROUND: Lateral flow assays (LFAs) are popular point-of-care diagnostic tools because they are rapid and easy to use. Nevertheless, they often lack analytical sensitivity and quantitative output and may be difficult to multiplex, limiting their usefulness in biomarker measurement. As a proof-of-concept study, we detail the design of a quantitative, multiplex LFA with readily available near-infrared (NIR) detection to improve analytical sensitivity.

METHODS: NIR dye was conjugated to selected antibodies and incorporated into LFAs. We used singleplex, optimized NIR-LFAs to measure interleukin (IL)-6 from 0 to 200 pg/mL and developed duplex assays to simultaneously measure IL-6 from 0 to 100 pg/mL (0 to 4.5 pmol/L) and C-reactive protein (CRP) from 50 to 2500 ng/mL (0.4 to 20 nmol/L) on a single test strip. Assays were tested on 60 different spiked samples and compared to ELISA results.

RESULTS: NIR-LFAs detected IL-6 in a 10% plasma matrix with a limit of detection of 4 pg/mL (182 fmol/L) and a CV <7%. Duplex NIR-LFAs quantitatively measured IL-6 and CRP concentrations simultaneously. Values strongly correlated to ELISA measurements, with R^2 values of 0.9825 and 0.9711 for IL-6 and CRP, respectively.

CONCLUSIONS: NIR-LFAs exhibit quantitative measurement at pg/mL concentrations owing to a high signal-to-background ratio and robust detection antibody clearance through the test strip. Moreover, NIR-LFAs are able to detect molecules present at vastly different concentrations in multiplex format and compare favorably to ELISAs. LFAs with direct NIR detection may be a valuable tool for biomarker evaluation in the point-of-care setting.

The use of point-of-care diagnostics for disease assessment and drug choice is rapidly expanding. Lateral flow assays (LFAs)[2] are popular point-of-care diagnostics originally developed for in-home measurement of human chorionic gonadotropin for pregnancy determination *(1)*. Now used in a variety of tests for drug screening, infective diseases, hormones, and cardiac and tumor markers, the LFA represents a fast, user-friendly diagnostic tool that requires minimal sample pretreatment *(2)*.

LFAs consist of a dried, preassembled test strip comprising immobilized capture and detection reagents (often antibodies) against analytes of interest. Fluid samples activate the test strip as they flow through the material. When capture and detection antibodies recognize the specific analyte in the fluid sample, a line forms on the membrane of the test strip *(2)*. The line may be read by the naked eye as occurs when the detection antibody is bound to colloidal gold, colloidal platinum, carbon nanoparticles, or dye-filled latex beads. However, these technologies have limited analytical sensitivity, yield qualitative results, and are subjective *(2)*.

To obtain quantitative results, desktop and handheld readers are now being used, and scientists are incorporating a wide range of new detection technologies. Whereas fluorescent nanoparticles, upconverting phosphors, and magnetic- and electroluminescent-based assays are becoming more popular, dye-conjugated antibodies (rather than a particle) have seen limited use due to their low signal-to-noise ratio. Ahn et al. *(3)* developed a C-reactive protein (CRP) test that used Alexa647 and a 1-dimensional fluorescent scanner. With direct mixing of detection antibody and sample, a limit of detection (LOD) of 0.133 mg/L was achieved *(3)*. Choi et al. *(4)* used the same approach to develop an LFA for serum albumin that achieved a detection range of 15–60 g/L. Although both of these assays boasted CVs <10%, their low analytical sensitivities make them inadequate to measure proteins present at low concentrations in test samples.

[1] SRI International, Menlo Park, CA.
* Address correspondence to the authors at: Christina Swanson or Annalisa D'Andrea, 333 Ravenswood Ave., Menlo Park CA 94025-3493; Fax 650-859-2000 or 650-859-3444; e-mail christina.swanson@sri.com or annalisa.dandrea@sri.com.

Received November 28, 2012; accepted January 15, 2013.
Previously published online at DOI: 10.1373/clinchem.2012.200360

[2] Nonstandard abbreviations: LFA, lateral flow assay; CRP, C-reactive protein; LOD, limit of detection; NIR, near-infrared; IL, interleukin; HRP, horseradish peroxidase; LOQ, limit of quantification.

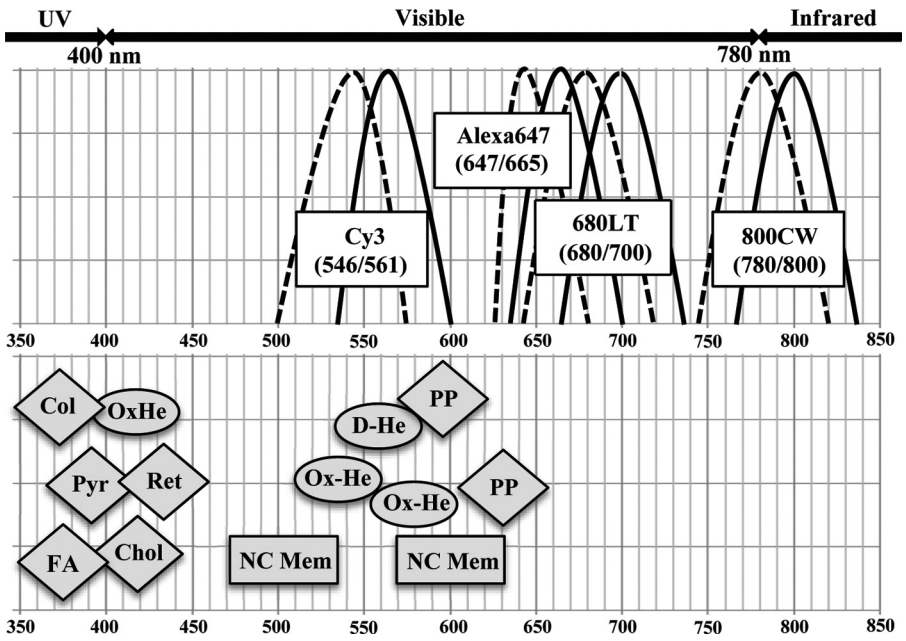

Fig. 1. Autofluorescent and absorbent agents in the UV, visible, and infrared regions.

Representative spectrums of Cy3, Alexa647, 680LT, and 800CW fluorescent dyes overlaid with autofluorescent and absorbent blood and nitrocellulose membrane components. Diamonds represent autofluorescent emission peaks of plasma/blood proteins including pyridoxine (Pyr), retinol A (Ret), collagen (Col), cholecalciferol (Chol), folic acid (FA), and porphyrin (PP); ovals represent absorbent peaks of oxy-hemoglobin (OxHe) and deoxy-hemoglobin (D-He); and rectangles represent autofluorescent peaks of nitrocellulose membrane (NC Mem).

The low analytical sensitivity of dye-conjugated antibodies can, in part, be attributed to high background in the visible region caused by autofluorescence of the membrane and sample matrix. Molecules in plasma such as NAD(P)H, pyridoxine (vitamin B_6), bilirubin, retinol (vitamin A), collagen, cholecalciferol, and folic acid autofluoresce in the 300- to 450-nm range *(5–10)*. Porphyrins in plasma autofluoresce at 590 and 630 nm, and nitrocellulose membranes autofluoresce at 500 and 600 nm *(11–13)*. In addition, oxyhemoglobin, which has maximal absorption peaks at 541 and 577 nm, and deoxy-hemoglobin, which has an absorption peak at 555 nm, may dampen dye emission intensity *(14)* (Fig. 1). These properties make fluorescent detectors with excitation/emission in the 300- to 650-nm range difficult to use, indicating a potential advantage in the use of dyes outside this wavelength range.

As proof of concept, we developed an LFA assay that takes advantage of near-infrared (NIR) dye detection (NIR-LFA). The International Organization for Standardization (ISO 20743:2007) defines the NIR region of the electromagnetic spectrum as 780 to 3000 nm. NIR dyes offer easy antibody conjugation and avoid the issues of the visual range such as background from test strip materials and biological fluids. Compared with LFAs that use fluorescent dyes in the ultraviolet and visible spectrum, NIR-LFAs offer superb analytical sensitivity, with detection of proteins in the low pg/mL range. In addition, NIR-LFAs are highly tunable, allowing detection of analytes at concentrations ranging from pg/mL to μg/mL. To this end, we constructed and optimized a multiplex LFA that simultaneously and accurately measured interleukin (IL)-6 and CRP in 10% human plasma on 1 test strip.

Materials and Methods

REAGENTS AND APPARATUS

Commercially available antibodies purchased included polyclonal goat anti-human IL-6 (R&D Systems), rat anti-human IL-6 (BD Biosciences), mouse anti-human CRP (R&D Systems), goat anti-mouse IgG (Millipore), and goat anti-rat horseradish peroxidase (HRP) (Invitrogen). Proteins purchased included human IL-6 (R&D Systems) and human CRP (Fitzgerald). We purchased buffer reagents, including BSA, sucrose, trehalose, sodium azide, Tween-20, NaCl, and polyvinyl py-

rolidone, from Sigma; HEPES from Gibco; and phosphate buffer from Calbiochem.

ANTIBODY DYE CONJUGATION

We conjugated antibodies to 800CW dye via an *N*-hydroxysuccinimide ester reactive group following standard protocols indicated in the IRDye® 800CW Microscale Protein Labeling Kit (Li-Cor Biosciences). Briefly, antibodies were diluted to 1 g/L in 50 mmol/L phosphate buffer, pH 7.0. We added potassium phosphate buffer at a ratio of 1:10 to increase the pH and dye at a dye-to-protein molar ratio of 3:1, and the contents were reacted for 2 h at room temperature. Dye-conjugated antibodies were purified via a 40-kDa desalting spin column (Pierce Zeba). We evaluated final antibody concentrations via a bicinchoninic acid protein assay kit (Pierce) and determined the dye-to-antibody ratio by comparing absorption at 785 nm against a calibration curve.

LFA PREPARATION

Capture reagents were diluted in buffer containing 10 mmol/L HEPES, 135 mmol/L NaCl, 20 g/L BSA, and 0.2 g/L sodium azide. Antibodies and protein were striped on a HF240 membrane (Millipore) at 1 μL/cm with an Ivek MicroStriper II. For the multiplex NIR-LFA, capture reagents were striped at the following specified distances past the conjugate release pad: 2 g/L goat-antihuman IL-6 at 9 mm, 1 g/L human CRP protein at 12 mm, 10 μg/mL goat anti-rat IgG-HRP at 27 mm, and 10 μg/mL goat anti-mouse IgG at 30 mm. Striped membranes were dried at 37 °C for 30 min and stored in a desiccator at <15% relative humidity until use.

We assembled the striped membrane, conjugate release pad, and absorbent pad together on the master card with 2-mm overlap between each component by use of a Kinematic Automation Matrix 2210 Universal Laminator Module. We cut the assembled card into 4-mm-wide strips with a Kinematic Automation Matrix 2360 Programmable Shear. 800CW-conjugated detection antibody was diluted to specified concentrations in dilution buffer consisting of 10 mmol/L HEPES, 50 g/L BSA, 50 g/L trehalose, 10 g/L polyvinyl pyrolidone, and Milli-Q water. Detection antibody solution (10 μL) was applied to the conjugate release pad of each test strip and dried for 1 h at 37 °C.

LFA ASSAY PROTOCOL

We diluted human plasma obtained from blood collected in EDTA tubes (Stanford Blood Bank) to 100 mL/L (10%) final concentration in a running buffer consisting of 10 mmol/L HEPES, 135 mmol/L NaCl, 5 mL/L Tween-20, and 0.2 g/L sodium azide. Plasma/buffer mixture (75 μL) was applied to the release pad of each test strip and allowed to run until completion. Test strips were either read wet after 15 min or allowed to dry completely and read.

IMAGE ACQUISITION AND DATA ANALYSIS

We visualized test strips by placing them face down on an Odyssey Li-Cor Scanner. They were scanned for emission with 1-mm focus offset and 42-μm resolution. Collected images were exported as tiff files and analyzed with ImageJ software (NIH). Briefly, we determined the raw integrated density inside rectangular areas at the target line and 1 mm upstream of the target line to determine the background intensity.

DOT-BLOT PREPARATION

Goat anti-rat 680LT (Li-Cor), goat anti-rat 800CW, plasma, blood, and indicated combinations were diluted in 1× PBS (8 mmol/L $Na_2HPO_4 \cdot 2\ H_2O$, 1.5 mmol/L KH_2PO_4, 137 mmol/L NaCl, 3 mmol/L KCl) (Life Technologies), and 0.8 μL of each mixture was spotted on nitrocellulose membrane HF240 (Millipore). Membranes were dried for 1 h at 37 °C and imaged with the Li-Cor Odyssey Scanner as indicated above.

MULTIPLEX NIR-LFA

Human plasma was diluted to 10% in running buffer and supplemented with different quantities of IL-6 (0–100 pg/mL) and CRP (0–2500 ng/mL). For each analyte, we determined a calibration curve with known concentrations of analyte for IL-6 and CRP from the singleplex data. We then compared intensity ratios for unknown samples to the calibration curve to determine analyte concentrations. Samples were run in quadruplicate.

ELISAs

Samples run on the multiplex NIR-LFA were analyzed directly by ELISA for human IL-6 (R&D Systems). Samples were diluted 50-, 500-, or 3000-fold to bring the samples into the appropriate assay range and analyzed by ELISA for human CRP (R&D Systems). All samples were run in quadruplicate.

STATISTICS

CVs were calculated as the SD divided by the mean. For differentiation of samples, we performed 2-tailed Student *t*-tests where indicated. The LOD was defined as mean + 3SD. The limit of quantification (LOQ) was defined as the mean + 10SD. We constructed Bland–Altman plots as the difference between the NIR-LFA and ELISA results vs the mean of the results.

Results

The analytical sensitivity of fluorescent dye–conjugated antibodies in LFAs is limited by high background from membrane/matrix autofluorescence and

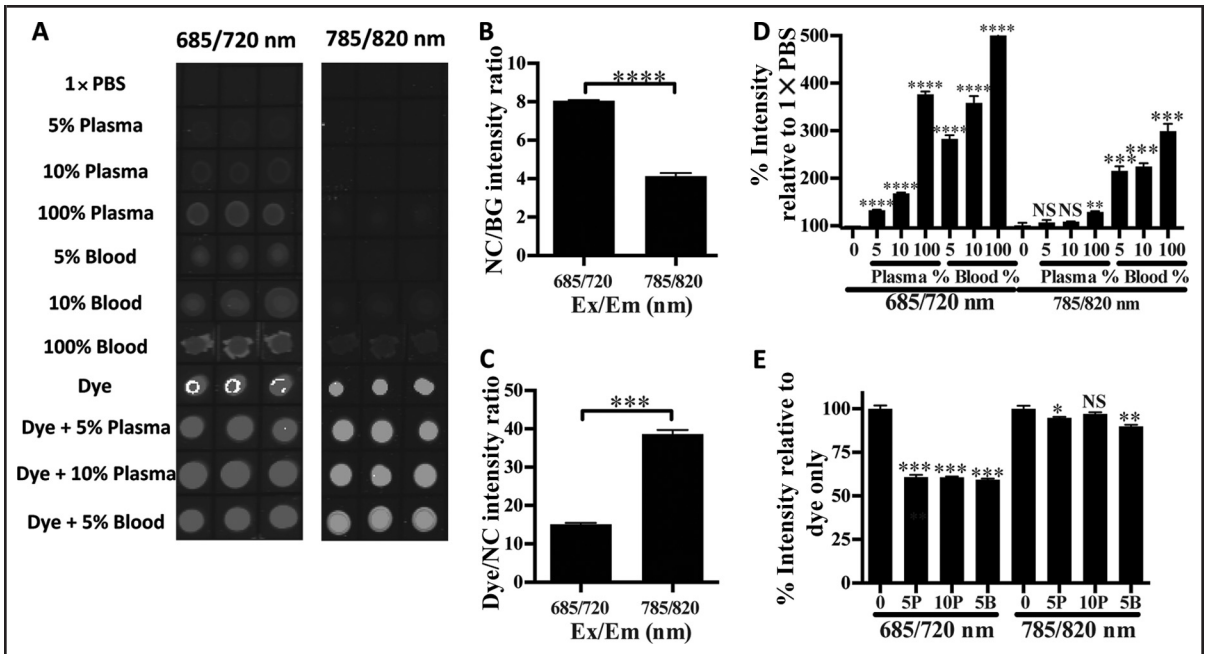

Fig. 2. (A), Images of dot-blots of plasma, blood, dye alone, and dye mixed with plasma/blood on nitrocellulose (NC) membrane.

(B), Quantification of nitrocellulose membrane versus background (BG) autofluorescence. (C), Signal-to-noise ratio of 680LT and 800CW dye spotted on nitrocellulose membrane. (D), Autofluorescence of plasma and blood spotted on nitrocellulose membrane. (E), Signal-dampening effect of 50 mL/L (5%) and 100 mL/L (10%) plasma (5P, 10P) and 50 mL/L (5%) blood (5B) when directly mixed with dye. (B–E) are representative of 2 experiments. Bars represent ± SE. Ex/Em, excitation/emission; NS, not significant. $*P < 0.05$, $**P < 0.01$, $***P < 0.001$, $****P < 0.0001$.

signal dampening from hemoglobin absorption (Fig. 1). To enhance the signal-to-noise ratio of fluorescent dye–conjugated antibodies in LFAs, we tested 2 dyes, 680LT and 800CW, in the NIR region with excitation wavelengths >650 nm. We spotted nitrocellulose membrane with buffer, dye, plasma, and blood at varying concentrations and measured the autofluorescence and signal dampening at excitation/emission peaks of 685/720 and 785/820 nm, respectively (Fig. 2A). Interestingly, nitrocellulose demonstrated significantly higher autofluorescence at 685/720 than at 785/820 nm (Fig. 2B). Because of this higher background, the ratio of the intensity of the dye spot to the background nitrocellulose was significantly higher for 800CW (Fig. 2C). Whereas plasma and blood showed bright autofluorescence at 685/720 nm, plasma autofluorescence was difficult to detect, and blood had a decreased fluorescence at 785/820 nm (Fig. 2D). When dye was mixed with plasma or blood, both matrices diminished the 680LT signal by nearly 40%, while reducing the 800CW signal by only 5–10% (Fig. 2E). Together, these data indicate that 800CW dye with excitation/emission peaks at 785/820 nm would work best in LFAs with plasma or blood. Although 800CW has been successfully used in Western blots, in vivo imaging, and microarrays, we believe that this is the first report of NIR dyes used in LFAs.

In humans, increased IL-6 is a biomarker of sepsis, cancer, and Alzheimer disease, among other conditions *(15–17)*. To demonstrate the analytical sensitivity of NIR-LFAs, we built a robust LFA to measure IL-6 concentrations in 10% plasma. The choice of 10% plasma was made to reduce the amount of plasma needed and enhance the flow of the sample in the assay. Our assay consisted of a conjugate release pad, nitrocellulose membrane, and absorbent pad all attached to backing (Fig. 3A). Membranes were striped with goat anti–IL-6 capture antibody at the target line and goat anti-rat IgG capture antibody at the control line. Dye-conjugated rat anti–IL-6 antibody was dried on the conjugate release pad. Human plasma samples were diluted to 10% in running buffer, supplemented with IL-6 from 0 to 200 pg/mL (0–9 pmol/L), and applied to wick. Running time was ≤10 min.

The NIR-LFA for IL-6 was able to readily differentiate values of IL-6 from 0 to 200 pg/mL with a signal-

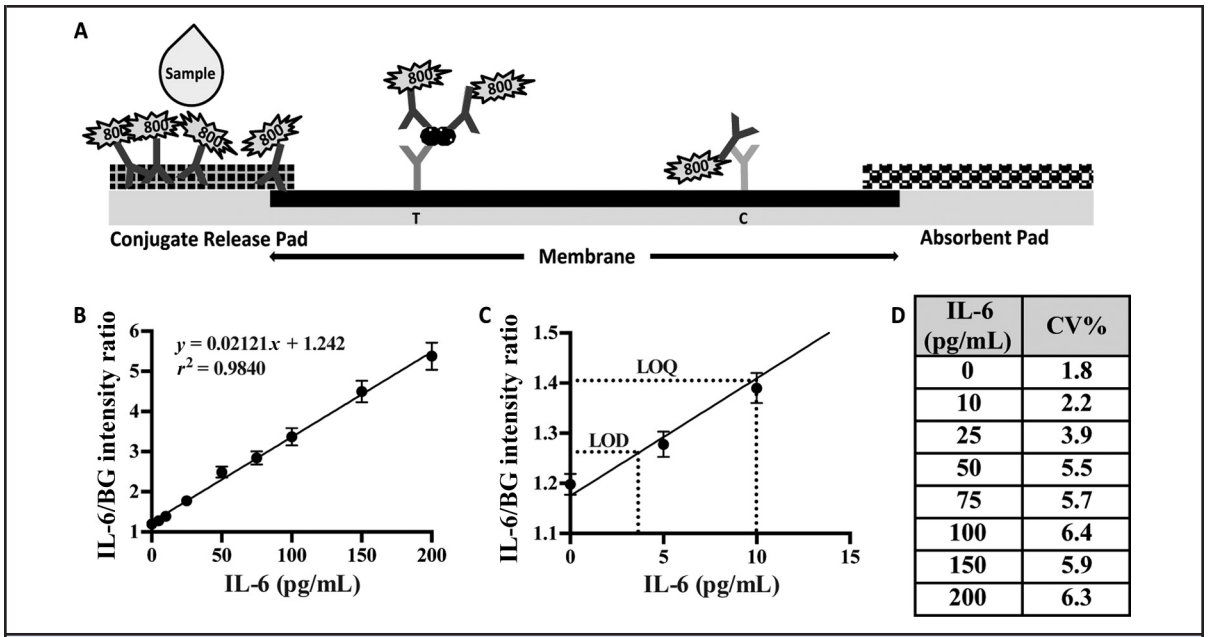

IL-6 (pg/mL)	CV%
0	1.8
10	2.2
25	3.9
50	5.5
75	5.7
100	6.4
150	5.9
200	6.3

Fig. 3. (A), Diagram of the test strip layout with target (T) and control (C) lines.

(B), Plasma samples spiked with IL-6 were measured in quintuplicate via NIR-LFA. The intensity ratio of IL-6 to background is plotted vs the spiked IL-6 concentration. Bars represent SD. (C), Zoomed-in version of (B) plotted from 0 to 15 pg/mL showing the calculated LOD and LOQ. (D), Intraexperiment CV% was calculated for each IL-6 concentration. (B)–(D) are representative of >3 experiments.

to-noise ratio >5.0 at 200 pg/mL (Fig. 3, B and C). Emission intensities closely followed a linear distribution, with the equation $y = 0.02121x + 1.242$ and $R^2 = 0.9840$ (Fig. 3B). The LOD was approximately 4 pg/mL (182 fmol/L), and the LOQ was 10 pg/mL (455 fmol/L) (Fig. 3C). Intraassay CVs were calculated for each concentration of IL-6 (Fig. 3D). CVs over the entire range of IL-6 concentrations were <7%.

Whereas the IL-6 concentration in blood can range from 0.1 to >1000 pg/mL *(18, 19)*, other popular biomarkers are considerably more abundant. CRP is a biomarker of cardiovascular risk, infection, trauma, tissue necrosis, autoimmunity, and some cancers *(20)*. Serum from healthy patients normally contains <10 mg/L CRP; however, this lower range may be further stratified to predict the relative risk for future coronary events *(21)*. CRP concentrations >15 mg/L indicate infection, and during severe bacterial infection CRP concentrations can increase 50 000-fold to >200 mg/L *(22)*.

To evaluate the flexibility of our NIR-LFA platform, we created a multiplex LFA that could simultaneously measure IL-6 and CRP in human plasma at a single 10% dilution. In the development of our duplex assay, we aimed to create a high-sensitivity assay that could accurately measure CRP concentrations in healthy subjects as well as patients at high risk of cardiovascular events or infection.

To develop a duplex NIR-LFA, we added a target and control line for measurement of CRP to the IL-6 NIR-LFA described above. Given the wide range of CRP concentrations in healthy and sick patients, from 0.05 to >200 mg/L, we chose an inhibition-style assay rather than a sandwich-style assay to avoid complications due to a potential hook effect at high CRP concentrations. With this approach, free CRP present in the sample inhibited binding of the dye-conjugated antibody to CRP striped on the membrane. As the concentration of CRP in the sample increases, the signal directly decreases.

For our multiplex NIR-LFA, we diluted human plasma to 10% in running buffer and supplemented samples with 6 different IL-6 concentrations [0–100 pg/mL (0–4.5 pmol/L)] and 10 different CRP concentrations [0–2500 ng/mL (0–19.9 nmol/L)] in a grid pattern to create 60 different samples. These concentrations were chosen to cover the concentration ranges of IL-6 and CRP found in 10% plasma in healthy and septic patients. All samples were run in quadruplicate. We plotted the individual concentration curves achieved for IL-6 at every CRP concentration (Fig. 4A) and for CRP at every IL-6 concentration (Fig. 4B). IL-6

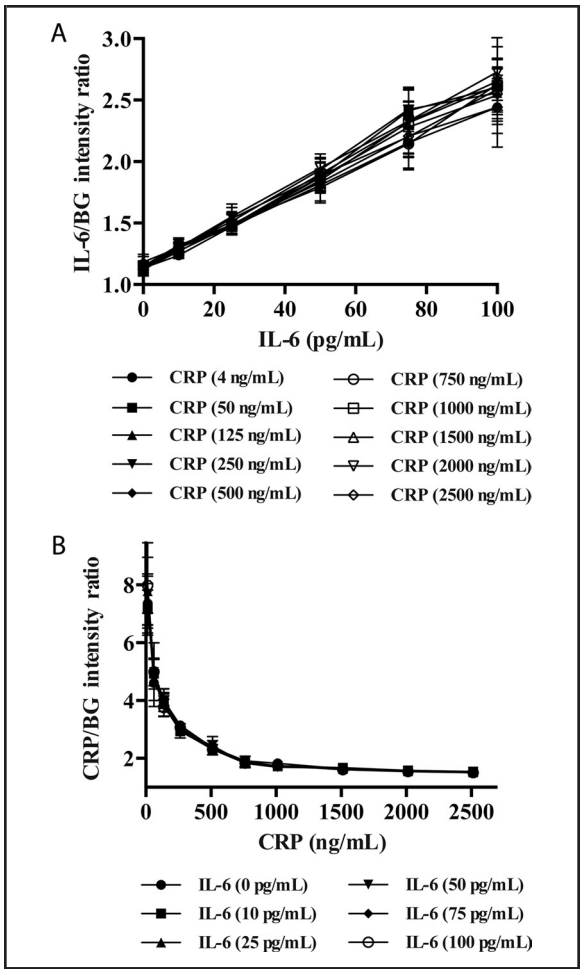

Fig. 4. Duplex NIR-LFA, simultaneous measurement of CRP and IL-6.

(A), Intensity ratio of IL-6 to background line plotted for every concentration of IL-6 over the entire CRP range. (B), Intensity ratio of CRP to background line plotted for every CRP concentration over the entire IL-6 range. Representative of 2 experiments. Bars represent ± SD.

emission intensity followed a linear distribution (Fig. 4A). Further, SDs correlated with brightness, increasing with higher concentrations of IL-6 and lower concentrations of CRP (Fig. 4, A and B).

Individual ELISAs are often used to measure concentrations of IL-6 and CRP in human plasma. To compare results obtained from NIR-LFAs to those of ELISAs, we measured the concentrations of IL-6 and CRP via ELISA in the same 60 samples that we applied to the LFAs above. IL-6 and CRP values were calculated in pg/mL and ng/mL, respectively, from the intensity ratio for every sample by use of the calibration curves generated for IL-6 alone and CRP alone. Figure 5, A and B, shows the mean value of quadruplicates for every sample as measured by ELISA or LFA. LFA and ELISA results were strongly correlated, showing linear correlations of $y = 1.024x + 1.256$ and $y = 1.009x + 20.16$ with R^2 values of 0.9825 and 0.9711 for IL-6 and CRP, respectively.

To determine the agreement between the NIR-LFAs and ELISAs, we constructed Bland–Altman plots as the difference between ELISA and NIR-LFA results vs the mean of the results for every sample. The duplex NIR-LFA compared to the ELISA had a bias offset of −2.383 pg/mL with 95% limits of agreement (bias and 1.96 SD) from −12.74 to 7.970 pg/mL for IL-6 (Fig. 5C). For CRP, the bias was −28.37 ng/mL with 95% limits of agreement from −330.4 to 273.7 ng/mL (Fig. 5D).

Discussion

We developed an LFA system that takes advantage of the beneficial properties of NIR detection. Our NIR-LFA measured IL-6 concentrations in plasma with a LOD of 4 pg/mL and CVs <7%. Moreover, the NIR-LFA could easily accommodate measurement of a wide analyte detection range, as shown by detection of 2 proteins at extremely different concentrations in plasma—IL-6 and CRP—on the same test strip. Importantly, there was no interference between the 2 analytes. Further, upon measuring concentrations in 60 different spiked plasma samples, the duplex NIR-LFA and ELISA results were highly correlated.

Fluorescence-based LFAs have been reported previously. They include assays that use quantum dots *(23)*, photoluminescent nanocrystals *(24)*, europium (III) chelate–dyed polystyrene nanoparticles *(25)*, upconverting phosphors *(26)*, microspheres *(27)*, silica nanoparticles covalently labeled with lathanide chelates *(28)*, dye-filled latex beads *(29)*, and dye-conjugated antibodies *(3, 4)*. The NIR-LFA, however, has distinct advantages on several critical points. First, whereas the fluorescent assays reported have emission/excitation spectrums ranging from UV to 720 nm, with most in the 500- to 600-nm range *(3, 4, 23–25, 27–29)*, the NIR-LFA uses dye with excitation/emission peaks of 785/820 nm. Use of a dye in the NIR region helps increase the signal-to-noise ratio in plasma and blood by reducing the background from autofluorescent proteins and matrix materials and avoids possible dampening mediated by hemoglobin absorption.

Second, whereas LFAs have classically used particle-based detection methods, we directly conjugated 800CW dye to the detection antibody, an approach that allowed use of a membrane with a smaller pore size and slower flow rate and thus higher analytical sensitivity. Further, by using dye-conjugated antibodies, particle aggregation on the conjugate release pad and in the membrane itself was

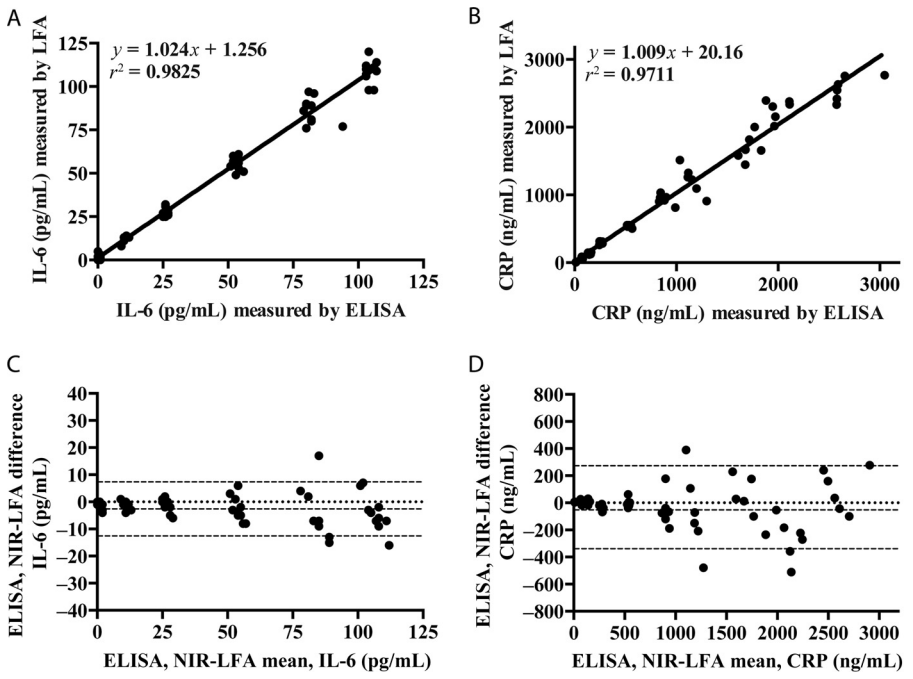

Fig. 5. Correlation of duplex NIR-LFA with ELISA.

Mean concentration of each sample as determined by NIR-LFA is plotted vs the value obtained by ELISA for IL-6 (A) and CRP (B). (C), NIR-LFA IL-6 measurement bias of −2.383 pg/mL and 95% limits of agreement from −12.74 to 7.970 pg/mL. (D), NIR-LFA CRP measurement bias of −28.37 ng/mL with 95% limits of agreement from −330.4 to 273.7 ng/mL. All results are representative of 2 experiments.

avoided. Finally, direct dye attachment provided an easy, fast, and reliable conjugation method that was controllable and quantifiable, making 800CW dyes potentially applicable to a wide range of assay types for antibodies, proteins, DNA, etc.

Finally, as a function of the other enhancements, the NIR-LFA enabled multiplexing of a wide range of analytes at different blood/plasma concentrations, as exemplified by the measurement of IL-6 and CRP on the same test strip, which are present in the blood at pg/mL and mg/L concentrations, respectively. To our knowledge, only 2 other fluorescence-based, multiplex LFAs have been reported in the literature, neither of which are simple procedures or use dye-conjugated antibodies. Worsley et al. *(27)* developed a single-line, multiplex LFA that used fluorescent microspheres, which measured IL-6 and IL-8 in plasma with LODs of 7.15 and 10.7 pg/mL, respectively. Likewise, Corstjens et al. *(26)* developed a multiplex LFA that used upconverting phosphors, which measured IL-10 and interferon-γ in assay buffer at concentrations from 1 to 100 pg/mL. Although both assays achieved high analytical sensitivity, they relied on conjugate–sample premixing, addition of a wash buffer, and in the case of IL-10/interferon-γ, separate mixing and addition of the different detection moieties to the test strip *(26, 27)*.

The NIR-LFA performed favorably compared to the LFA-based tests on the market. With an LOD of 4 pg/mL for IL-6 in 10% plasma, the NIR-LFA showed analytical sensitivity similar to that of the Milenia QuickLine IL-6 Rapid Immunochromographic Test, which has an LOD of 50 pg/mL in serum or plasma. However, whereas the QuickLine IL-6 test requires 100 μL sample and cannot be used with blood, the NIR-LFA requires only 7.5 μL plasma or serum and may be used with 5% blood. The NIR-LFA uses an inhibitory-style test to measure CRP (in 10% plasma) from 0.05 to 2.5 μg/mL, which represents 0.5 to 25 mg/L in whole plasma. One could envision the use of this approach for measurement of CRP in healthy people for cardiovascular risk assessment. Further, samples with CRP concentrations >25 mg/L (patients with severe infections) may be readily identified by the absence of signal. Thus, the NIR-LFA compares favorably to the NycoCard CRP test (Axis-Shield), which has a range of 5–120 mg/L for serum/plasma samples and involves multiple steps.

Although the NIR-LFA is analytically sensitive and easy to use, it currently faces several limitations for use

in a point-of-care setting. Foremost, a commercial handheld test strip reader is not presently available to read test strips with infrared dye. Second, our current IR800-LFA requires plasma to be diluted externally to 10% and then added to the test strip, creating an unnecessary step. Improvements could include either the addition of a plasma separation membrane to the test strip itself or an external plasma filtration device.

In conclusion, we report here the use of NIR dye directly conjugated to antibody as a successful detection moiety to measure IL-6 and CRP in the LFA format. 800CW dye is a particularly good choice for detection in LFAs because it has strong emission under ambient conditions, is excited by cheap and readily available 785-nm lasers, is easily conjugated to proteins, and is monodisperse, thus avoiding aggregation issues. To our knowledge, this is the first report of a multiplex LFA that uses both sandwich and inhibitory assays on the same test strip with a detection range of nearly 5 orders of magnitude. This NIR-LFA is a simple test, requires only 7.5 μL of plasma, demonstrates high analytical sensitivity, and correlates with ELISA results.

Author Contributions: *All authors confirmed they have contributed to the intellectual content of this paper and have met the following 3 requirements: (a) significant contributions to the conception and design, acquisition of data, or analysis and interpretation of data; (b) drafting or revising the article for intellectual content; and (c) final approval of the published article.*

Authors' Disclosures or Potential Conflicts of Interest: *No authors declared any potential conflicts of interest.*

Role of Sponsor: No sponsor was declared.

Acknowledgments: We thank Kenneth Shew for originally training us to use the LFA manufacturing equipment. Members of the cancer group were most helpful in letting us use their Li-Cor Odyssey Scanner. Fangfang Yin provided valuable feedback on this project.

References

1. Wong R, Tse H, eds. Lateral Flow Immunoassay. New York: Humana Press; 2009.
2. Posthuma-Trumpie GA, Korf J, van Amerongen A. Lateral flow (immuno)assay: its strengths, weaknesses, opportunities and threats. A literature survey. Anal Bioanal Chem 2009;393:569–82.
3. Ahn JS, Choi S, Jang SH, Chang HJ, Kim JH, Nahm KB, et al. Development of a point-of-care assay system for high-sensitivity C-reactive protein in whole blood. Clin Chim Acta 2003;332:51–9.
4. Choi S, Choi EY, Kim DJ, Kim JH, Kim TS, Oh SW. A rapid, simple measurement of human albumin in whole blood using a fluorescence immunoassay (I). Clin Chim Acta 2004;339:147–56.
5. Bondza-Kibangou P, Millot C, Dufer J, Millot JM. Modifications of cellular autofluorescence emission spectra under oxidative stress induced by 1 alpha,25dihydroxyvitamin D(3) and its analog EB1089. Technol Cancer Res Treat 2004;3:383–91.
6. Croce AC, De Simone U, Freitas I, Boncompagni E, Neri D, Cillo U, et al. Human liver autofluorescence: an intrinsic tissue parameter discriminating normal and diseased conditions. Lasers Surg Med 2010;42:371–8.
7. Katz ML, Eldred GE, Robison WG. Lipofuscin autofluorescence: evidence for vitamin A involvement in the retina. Mech Ageing Dev 1987;39:81–90.
8. Burkhardt M, Vollmar B, Menger MD. In vivo analysis of hepatic NADH fluorescence: methodological approach to exclude Ito-cell vitamin A-derived autofluorescence. Adv Exp Med Biol 1998;454:83–9.
9. Haga Y, Kay HD, Tempero MA, Zetterman RK. Flow cytometric measurement of intracellular bilirubin in human peripheral blood mononuclear cells exposed to unconjugated bilirubin. Clin Biochem 1992;25:277–83.
10. Thomas AH, Lorente C, Capparelli AL, Pokhrel MR, Braun AM, Oliveros E. Fluorescence of pterin, 6-formylpterin, 6-carboxypterin and folic acid in aqueous solution: pH effects. Photochem Photobiol Sci 2002;1:421–6.
11. Masilamani V, Al-Zhrani K, Al-salhi M, Al-Diab A, Al-Ageily M. Cancer diagnosis by autofluorescence of blood components. J Lumin 2004;109:143–54.
12. Walter JG, Stahl F, Reck M, Praulich I, Nataf Y, Hollas M, et al. Protein microarrays: reduced autofluorescence and improved LOD. Eng Life Sci 2010;10:103–8.
13. Jia Z, Wan X. Concentration of protoporphyrin IX in cancer tissues and blood in patients with colorectal cancer at early stage. J Cent South Univ 2009;34:846–9.
14. Zeng H, MacAulay C, McLean DI, Palcic B. Reconstruction of in vivo skin autofluorescence spectrum from microscopic properties by Monte Carlo simulation. J Photochem Photobiol B 1997;38:234–40.
15. Woiciechowsky C, Schöning B, Cobanov J, Lanksch WR, Volk HD, Döcke WD. Early IL-6 plasma concentrations correlate with severity of brain injury and pneumonia in brain-injured patients. J Trauma 2002;52:339–45.
16. Swardfager W, Lanctôt K, Rothenburg L, Wong A, Cappell J, Herrmann N. A meta-analysis of cytokines in Alzheimer's disease. Biol Psychiatry 2010;68:930–41.
17. Smith PC, Hobisch A, Lin DL, Culig Z, Keller ET. Interleukin-6 and prostate cancer progression. Cytokine Growth Factor Rev 2001;12:33–40.
18. Ten Oever J, Tromp M, Bleeker-Rovers CP, Joosten LA, Netea MG, Pickkers P, et al. Combination of biomarkers for the discrimination between bacterial and viral lower respiratory tract infections. J Infect 2012;65:490–5.
19. Sripa B, Thinkhamrop B, Mairiang E, Laha T, Kaewkes S, Sithithaworn P, et al. Elevated plasma IL-6 associates with increased risk of advanced fibrosis and cholangiocarcinoma in individuals infected by Opisthorchis viverrini. PLoS Negl Trop Dis 2012;6:e1654.
20. Volanakis JE. Human C-reactive protein: expression, structure, and function. Mol Immunol 2001;38:189–97.
21. Rifai N, Ridker PM. High-sensitivity C-reactive protein: a novel and promising marker of coronary heart disease. Clin Chem 2001;47:403–11.
22. Simon L, Gauvin F, Amre DK, Saint-Louis P, Lacroix J. Serum procalcitonin and C-reactive protein levels as markers of bacterial infection: a systematic review and meta-analysis. Clin Infect Dis 2004;39:206–17.
23. Yang H, Li D, He R, Guo Q, Wang K, Zhang X, et al. A novel quantum dots–based point of care test for syphilis. Nanoscale Res Lett 2010;5:875–81.
24. Shen H, Yuan H, Niu JZ, Xu S, Zhou C, Ma L, et al. Phosphine-free synthesis of high-quality reverse type-I ZnSe/CdSe core with CdS/Cd(x)Zn(1 – x)S/ZnS multishell nanocrystals and their application for detection of human hepatitis B surface antigen. Nanotechnology 2011;22:375602.
25. Juntunen E, Myyryläinen T, Salminen T, Soukka T, Pettersson K. Performance of fluorescent europium(III) nanoparticles and colloidal gold reporters in lateral flow bioaffinity assay. Anal Biochem 2012;428:31–8.
26. Corstjens PL, de Dood CJ, van der Ploeg-van Schip JJ, Wiesmeijer KC, Riuttamäki T, van Meijgaarden KE, et al. Lateral flow assay for simultaneous detection of cellular- and humoral immune responses. Clin Biochem 2011;44:1241–6.
27. Worsley GJ, Attree SL, Noble JE, Horgan AM. Rapid duplex immunoassay for wound biomarkers at the point-of-care. Biosens Bioelectron 2012;34:215–20.
28. Xia X, Xu Y, Zhao X, Li Q. Lateral flow immunoassay using europium chelate-loaded silica nanoparticles as labels. Clin Chem 2009;55:179–82.
29. Nabatiyan A, Baumann MA, Parpia Z, Kelso D. A lateral flow-based ultra-sensitive p24 HIV assay utilizing fluorescent microparticles. J Acquir Immune Defic Syndr 2010;53:55–61.